Electronic Properties of Cu/*n*-InP Metal–Semiconductor Structures with Cytosine Biopolymer

Ö. Güllü[a,*] and A. Türüt[b]

[a]Batman University, Faculty of Sciences and Arts, Department of Physics, Batman, Turkey

[b]Istanbul Medeniyet University, Faculty of Sciences, Department of Engineering Physics, 34000 Istanbul, Turkey

(Received January 5, 2015; revised version June 3, 2015; in final form June 11, 2015)

This work shows that cytosine biomolecules can control the electrical characteristics of conventional Cu/*n*-InP metal–semiconductor contacts. A new Cu/*n*-InP Schottky junction with cytosine interlayer has been formed by using a drop cast process. The current–voltage (I–V) and capacitance–voltage (C–V) characteristics of Cu/cytosine/*n*-InP structure were investigated at room temperature. A potential barrier height as high as 0.68 eV has been achieved for Cu/cytosine/*n*-InP Schottky diodes, which have good I–V characteristics. This good performance is attributed to the effect of interfacial biofilm between Cu and *n*-InP. By using C–V measurement of the Cu/cytosine/*n*-InP Schottky diode the diffusion potential and the barrier height have been calculated as a function of frequency. Also, the interface-state density of the Cu/cytosine/*n*-InP diode was found to vary from 2.24×10^{13} eV^{-1} cm^{-2} to 5.56×10^{12} eV^{-1} cm^{-2}.

DOI: 10.12693/APhysPolA.128.383

PACS: 73.40.–c, 73.30.+y

1. Introduction

Recently, devices based on biomaterials have been investigated by several authors with great interest [1–7]. Among them, nucleic acids and their derivatives attract a lot of attention of researchers due to their important biological role [8]. At the same time deoxyribonucleic acid (DNA), which exhibits a charge migration, is a subject of interest for its physical properties, and particularly for a great potential of application in photonics and in molecular electronics. Such applications include: devices based on second and third order nonlinear optical effects [9], low loss optical waveguides [10], holography [11, 12], organic photovoltaics and organic field effect transistors (FET) [13].

The nucleic base of DNA is 0.34 nm long with a diameter of the helix about 2 nm. Therefore, the double helix with a π–π^* stacking structure of nucleobase pairs of DNA forms a tunnel suitable for electron transfer. The relatively weak π–π^* electron conjugation renders materials with a large optical transparency window [8]. Although its first historic measurement was reported in 1962 [14, 15], the electrical conductivity of DNA has become a hot topic only from the last decade. The great interest in electrical conduction of DNA is its possible application as a material to fabricate different nanometer scale electronic devices due to its sequence-specific molecular recognition and its special structure with self-assembling capabilities [16–18].

To explain the electrical conductivity of DNA, several mechanisms have been developed. These mechanisms include single-step superexchange, multistep hole hopping, phonon-assisted polaron hopping, and molecular band conduction model [15]. In spite of these different mechanisms, electron transport through DNA molecules has been recognized to proceed along a one-dimensional pathway made up of the overlap between π orbitals in neighboring base pairs [14]. This is because effective electron transport requires conjugated molecular chains such as π-orbital overlap to form a pathway. Although charge transfer can be conducted along a path constituted with σ-orbital overlap, this charge transfer can proceed only at a very short distance [19].

The basic unit of a DNA molecule (please see Fig. 1), nucleotide, is a molecule composed of a pentose sugar bonded to both a phosphate group and a nitrogen-containing heterocyclic base that may be adenine (A), guanine (G), cytosine (C), or thymine (T). The DNA double helix structure is formed when two single strands combine together through hydrogen bonds of the complementary A–T and G–C base pairs. It is the π stacking of the conjugated base pairs that not only stabilizes the helix but also constitutes the pathway for electron transport [15, 20, 21].

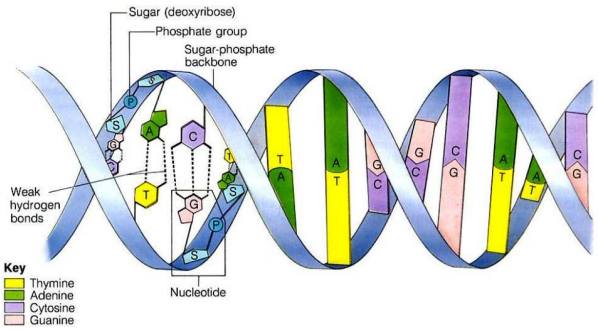

Fig. 1. Double helix structure of DNA.

*corresponding author; e-mail: omergullu@gmail.com

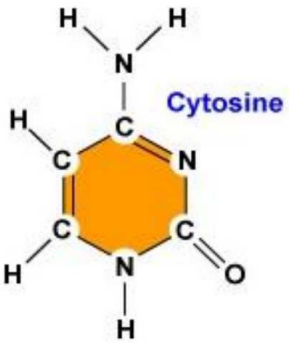

Fig. 2. Chemical structure of cytosine.

Additionally, cytosine (please see Fig. 2) is a pyrimidine derivative, with a heterocyclic aromatic ring and two substituents attached. It has a chemical formula of $C_4H_5N_3O$ and a molecular weight of 111.10 atomic mass units. Cytosine was first discovered in 1894 when it was isolated from calf thymus tissues. A structure was proposed in 1903, and was synthesized (and thus confirmed) in the laboratory in the same year [22, 23].

InP is one of the most promising semiconducting materials for microwave and optoelectronic devices [24], but it has a major disadvantage of low Schottky barrier height (SBH) [10]. This inherently low SBH (0.40–0.45 eV) makes it difficult to fabricate FETs directly on InP because of the serious leakage current problem through the gate electrode [25]. Effort has been devoted to forming InP Schottky junctions with a high barrier [26]. One method for enhancing the effective Schottky barrier height is to form a tunnel metal–interlayer–semiconductor (MIS) structure [27–29]. An enhancement of the barrier height up to 0.7–0.8 eV has been achieved by fabricating MIS Schottky junctions [26]. Another method is to release the surface Fermi level pinning and use a high work function metal [30]. Assuming that the surface Fermi level pinning is caused by high surface state density, passivation technology is needed to reduce the surface states of InP. To fabricate MIS Schottky diodes with an enhanced barrier height, it is useful to develop an *in situ* process in which surface passivation and insulating film deposition are carried out successively [24].

New electrical properties of the MS contacts can be promoted by means of the choice of suitable organic molecules [31, 32]. In this study, we will fabricate the Cu/cytosine/n-InP MIS device by a drop cast method. Cytosine biomolecules have been considered as one of the most stable organic materials for various electronic and optoelectronic applications and has not been used for the modification of n-InP diodes. Our aim is to investigate the electrical properties of Cu/cytosine/n-InP MIS diode by the insertion of cytosine organic layer between n-InP semiconductor and Cu metal by using current–voltage (I–V) and capacitance–voltage (C–V) measurements and is to compare the electrical parameters of the Cu/cytosine/n-InP MIS diode with those of conventional (reference) MS diodes.

2. Experimental details

MIS structure was prepared using one side polished (as received from the manufacturer) n-type InP wafer in this study. The wafer was chemically cleaned with $3H_2SO_4{+}H_2O_2{+}H_2O$ (a 20 s boil). The native oxide on the front surface of n-InP was removed in a HF:H_2O (1:10) solution and finally the wafer was rinsed in deionized (DI) water for 30 s. Before forming cytosine biopolymer layer on n-InP substrate, the ohmic contact was made by evaporating indium metal on the back of the substrate, followed by a temperature treatment at 350 °C for 60 s in N_2 atmosphere.

High purity (≈99%) cytosine powder was purchased from MWG Biotech AG (Ebersberg, Germany). After the cleaning procedures and ohmic metallization were carried out, cytosine thin film was directly formed by adding 10 μL cytosine solution with concentration of 200 μg/ml in deionised water on the front surface of the n-InP wafer, and evaporated by itself for drying of solvent in N_2 atmosphere for two days. Here, we selected an amount of 10 μL of the cytosine solution by considering and testing various factors that could effect a given cytosine film thickness and homogeneity depending on the solution concentration and substrate area. The quality of organic thin films should be also related to other factors, such as the film-forming ability, the molecular symmetry and structure [33]. The contacting top metal dots with diameter of 1.0 mm were formed by evaporation of Cu metal. We also fabricated Cu/n-InP reference diode without the organic layer to compare with the electrical parameters of the Cu/cytosine/n-InP device. All evaporation processes were carried out in a vacuum coating unit at about 10^{-5} mbar.

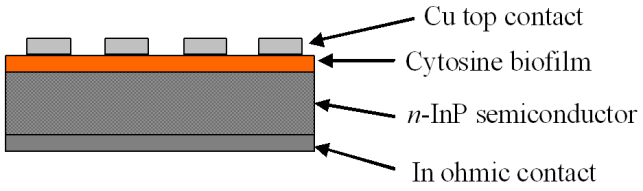

Fig. 3. A schematic cross-section of the Cu/cytosine/n-InP structure.

The I–V and C–V measurements of Cu/cytosine/n-InP structure (please see Fig. 3) were performed by KEITLEY 487 Picoammeter/Voltage Source and HP 4192A (50 Hz–13 MHz) LF impedance analyzer, respectively.

3. Results and discussion

Current transport in the Schottky contacts may be described by thermionic emission (TE) over the interface barrier [34]. The thermionic current can be written as

$$I = I_0 \left[\exp\left(\frac{qV}{nkT}\right) - 1 \right], \tag{1}$$

where V is the applied voltage, n is the ideality factor and I_0 is the saturation current determined by

$$I_0 = AA^*T^2 \exp\left(-\frac{\Phi_b}{kT}\right), \tag{2}$$

where A is the diode area, A^* is the effective Richardson constant, k is the Boltzmann constant, T is the absolute temperature, q is the electron charge and Φ_b is the barrier height. From Eqs. (1) and (2), ideality factor n and barrier height Φ_b can be written as

$$n = \frac{q}{kT}\left(\frac{dV}{d\ln I}\right) \tag{3}$$

and

$$\Phi_b = kT \ln\left(\frac{AA^*T^2}{I_0}\right), \tag{4}$$

respectively.

Figure 4 shows the experimental semi-log I–V characteristics of the Cu/n-InP reference diode and the Cu/cytosine/n-InP Schottky device at room temperature. As clearly seen from Fig. 4, the Cu/cytosine/n-InP Schottky structure shows a good rectifying property. The weak voltage dependence of the reverse-bias current and the exponential increase of the forward-bias current are characteristic properties of rectifying interfaces. The current curve in forward bias quickly becomes dominated by series resistance (R_s) from contact wires or bulk resistance of the organic interlayer and inorganic semiconductor, giving rise to the curvature at high current in the semi-log I–V plot. This figure indicates that the leakage current of the Cu/cytosine/n-InP Schottky device decreases in a significant rate like more than about three orders of magnitude with respect to that of MS reference Schottky diode without cytosine interlayer.

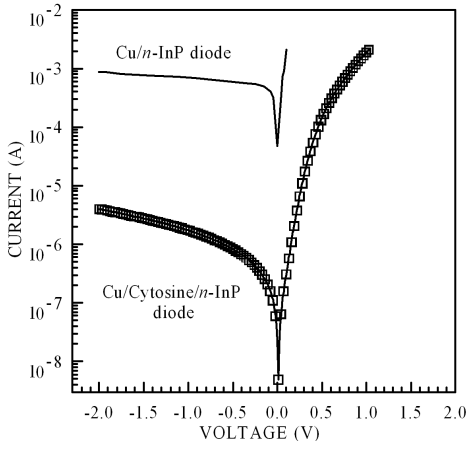

Fig. 4. Current-voltage characteristics of the Cu/cytosine/n-InP MIS device and a reference Cu/n-InP MS diode at room temperature and in dark.

By using TE theory [34], the ideality factor and BH (Φ_b) can be obtained from the slope and the current axis intercept of the linear region of the forward bias I–V plot, respectively. The values of the BH and the ideality factor for the Cu/cytosine/n-InP diode have been calculated as 0.68 eV and 1.68, respectively. The ideality factor determined by the image-force effect alone should be close to 1.01 or 1.02 [34–37].

The barrier height value of 0.68 eV calculated for the Cu/cytosine/n-InP contact is much higher than value of 0.45 eV for Cu/n-InP conventional diode shown in Fig. 4. This value appears to be one of the highest barrier values ever reported for the metal/n-InP diodes modified by an organic interlayer. For example, Jones et al. [36] reported a Φ_b value of about 0.87 eV for poly(pyrrole)/n-InP structure. Also, Sugino et al. [25] reported a Φ_b value of 0.78 eV for Au/n-InP MIS devices, and Sakamoto et al. [24] obtained a value of 0.83 eV for Au/n-InP MIS structure with PN_x interlayer. The findings indicate that the cytosine biofilm formed on n-InP inorganic substrate has modified the Φ_b value of MS n-InP Schottky diode in significant rate by influencing the space charge region of the inorganic substrate [19, 38].

Thereby, it is known that the cytosine organic thin film forms a physical barrier between the metal and the n-InP substrate, preventing the metal from directly contacting the InP surface [37, 39–42]. According to Roberts and Evans [38], the change in the Φ_b in the Cu/cytosine/n-InP device could be attributed to the substrate band bending originating from the cytosine organic thin interlayer.

It is well known that the downward concave curvature of the forward bias current–voltage plots at sufficiently large voltages is caused by the presence of series resistance, apart from the interface states, which are in equilibrium with the semiconductor [37, 40–43]. The R_s values have been calculated by using a method developed by Norde [44]. The following function has been defined in the modified Norde method [44]:

$$F(V) = \frac{V}{\gamma} - \frac{kT}{q}\ln\left(\frac{I(V)}{AA^*T^2}\right), \tag{5}$$

where γ is the first integer (dimensionless) greater than n. $I(V)$ is current obtained from the I–V curve. Once the minimum of the F vs. V plot is determined, the value of barrier height can be obtained from Eq. (6), where $F(V_0)$ is the minimum point of $F(V)$ and V_0 is the corresponding voltage

$$\Phi_b = qF(V_0) + \frac{qV_0}{\gamma} - kT. \tag{6}$$

Figure 5 shows the $F(V)$–V plot of the junction. From the Norde functions, R_s value can be determined as

$$R_s = \frac{kT(\gamma - n)}{qI_0}. \tag{7}$$

From the F–V plot by using $F(V_0) = 0.66$ V and $V_0 = 0.23$ V values, the values of Φ_b and R_s of the Cu/cytosine/n-InP structure have been determined as 0.75 eV and 1.81 kΩ, respectively. There is a difference between the Φ_b values obtained from the forward bias ln$I$–V and Norde functions.

For the Schottky structures having interface states in equilibrium with the semiconductor the ideality factor n becomes greater than unity as proposed by Card and

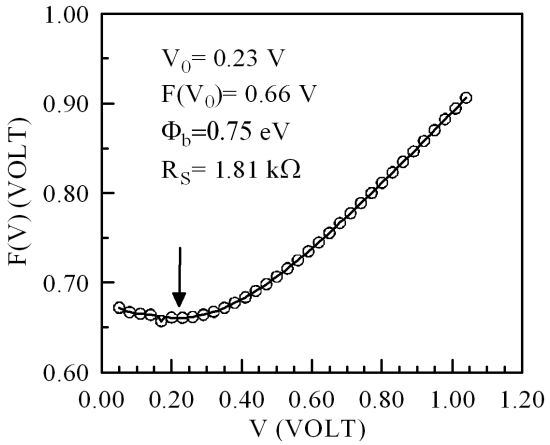

Fig. 5. $F(V)$ vs. V plot of the Cu/cytosine/n-InP MIS device.

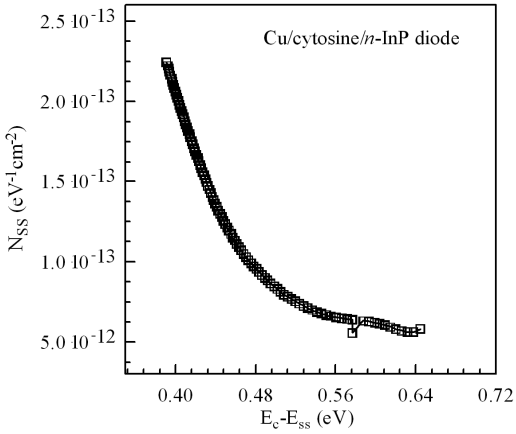

Fig. 6. $N_{\rm ss}$ vs. $E_{\rm c}-E_{\rm ss}$ plot of the Cu/cytosine/n-InP MIS device.

Rhoderick [45] and then the interface state density $N_{\rm ss}$ is given by

$$N_{\rm ss}=\frac{1}{q}\left[\frac{\varepsilon_{\rm i}}{\delta}(n(V)-1)-\frac{\varepsilon_{\rm s}}{d}\right], \tag{8}$$

where d is the space charge width, $\varepsilon_{\rm s}$ is the permittivity of the semiconductor, $\varepsilon_{\rm i}$ is the permittivity of the interfacial layer, δ is the thickness of the organic layer, and $n(V)=\frac{V}{(kT/q)\ln(I/I_0)}$ is the voltage-dependent ideality factor. In n-type semiconductors, the energy of the interface states $E_{\rm ss}$ with respect to the bottom of the conduction band at the surface of the semiconductor is given by

$$E_{\rm c}-E_{\rm ss}=\Phi_{\rm b}-qV, \tag{9}$$

where V is the applied voltage drop across the depletion layer and $\Phi_{\rm b}$ is the effective barrier height. The energy distribution or density distribution curves of the interface states can be determined from experimental data of this region of the forward bias I–V plot.

Substituting the voltage dependent values of n and the other parameters in Eq. (8), the $N_{\rm ss}$ vs. $E_{\rm c}-E_{\rm ss}$ plot was obtained as shown in Fig. 6. Here, the values of $\varepsilon_{\rm i}$ and δ are 12.5 and about 800 nm, respectively. The value of δ has been determined by using C–V measurement at 10 kHz ($C=\varepsilon A/\delta$). It is seen that the interface state density $N_{\rm ss}$ has an exponential rise with bias from some above the midgap towards the top of the conduction band for the structure. In this structure, deposition of cytosine on the inorganic semiconductor can generate a large number of interface states at the semiconductor surface that strongly influence the properties of the device. When this structure is considered as a Schottky diode, the diode comprises a high-resistivity layer (the depletion layer) in series with a low-resistivity layer, which has its own capacitance and resistance [46].

The C–V measurement is one of the most popular electrical measurement techniques used to characterize a Schottky diode. It is convenient to examine C–V data for rectifying contacts by plotting C^{-2} vs. V for reverse bias. The capacitance is measured at different reverse bias values by superimposing an ac voltage on the dc voltage. When the dc voltage corresponds to a reverse bias, the differential capacitance represents the response of the depletion layer to the ac signal [47]. In simple Schottky barrier theory the capacitance of the barrier varies with applied reverse voltage V in such a way that a straight line is obtained if C^{-2} is plotted against V. This relation is given by the expression [34]:

$$\frac{1}{C^2}=\frac{2(V_{\rm d}+V)}{q\varepsilon_{\rm s}A^2N_{\rm d}}, \tag{10}$$

where $\varepsilon_{\rm s}$ is the dielectric constant of n-InP, $V_{\rm d}$ is the diffusion potential at zero bias and is determined from the extrapolation of the linear C^{-2}–V plot to the V axis. The value of barrier height can be calculated by the relation

$$\Phi_{\rm b}(C-V)=qV_{\rm d}+qV_n, \tag{11}$$

where V_n is the potential difference between the Fermi level and the bottom of the conduction band of n-InP and can be calculated by knowing the carrier concentration $N_{\rm d}$ and it is obtained from the following relation:

$$V_n=\frac{kT}{q}\ln\left(\frac{N_{\rm c}}{N_{\rm d}}\right), \tag{12}$$

where $N_{\rm c}=4.9\times10^{17}$ cm^{-3} is the effective density of states in the conduction band [28].

Figure 7 shows the C–V characteristics of the Cu/cytosine/n-InP structure at various frequencies. As shown in Fig. 7, all C–V curves have a peak due to series resistance and interface layer effects. Also, it can be seen from this figure that at low frequencies the values of capacitance are shown to increase. The dependence of the capacitance of a rectifying contact upon frequency can also arise due to the presence of deep lying impurities in the depletion region of semiconductor. Deep impurities are energy levels of intrinsic lattice defects or impurity atoms that have energy near the center of the band gap. Presence of deep traps in the depletion region of the Schottky barrier makes the junction capacitance a complicated function of the bias voltage

and the measuring frequency. Also, it is observed that the low-frequency capacitance increases with the applied bias while the high-frequency capacitance remains almost constant. This observation may be attributed to the capacitive response of interface states to the measurement frequency. In general, at sufficiently high frequencies ($f > 500$ kHz) the interface states do not contribute to the capacitance [47, 48].

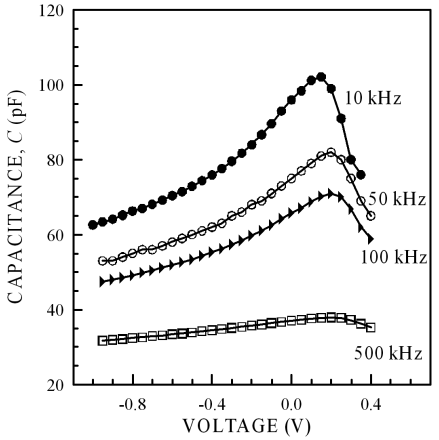

Fig. 7. C–V characteristic of the Cu/cytosine/n-InP MIS capacitor as a function of frequency.

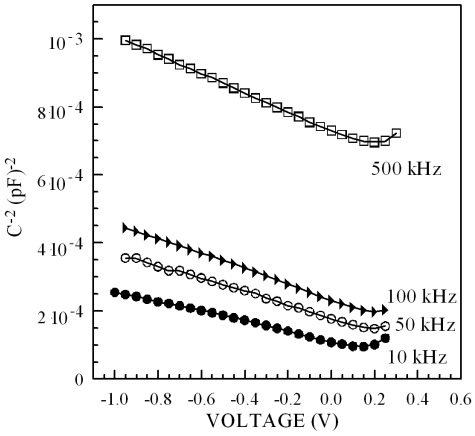

Fig. 8. C^{-2}–V characteristic of the Cu/cytosine/n-InP MIS capacitor as a function of frequency.

Figure 8 shows the reverse bias C^{-2}–V characteristics of the Cu/cytosine/n-InP structure at various frequencies. The C^{-2} plots as a function of reverse bias voltage are linear which indicates the formation of the Schottky junction. As can be seen from Fig. 8, the slopes of C^{-2} vs. V curves decrease with increase of frequency. This case may be explained by the charges at the interface states that follow an alternating-current signal.

Especially at lower frequencies, an important frequency dependence of C^{-2} vs. V is quite clear. This can be explained by taking into account the series resistance of the device [49]. It can be seen that all of these plots are nearly linear. This indicates that the formation of these structures resembles a Schottky diode and allows the use of the simple depletion layer theory (Eq. (10)) and the linearity in plot of C^{-2} vs. V indicates that the charge density within the depletion region of the structure is uniform. Some parameters of the structure are listed in Table by using the reverse bias C^{-2}–V characteristics. As can be seen in Table, the values of the diffusion potentials and Fermi energy levels tend to increase towards the high frequencies.

TABLE

Some parameters obtained for Cu/cytosine/n-InP diode by using reverse bias C^{-2}–V characteristics as a function of frequency.

f [kHz]	$V_{\rm d}$ [V]	$N_{\rm d} \times 10^{14}$ [cm^{-3}]	V_n [V]	$\Phi_{\rm b}$ [eV]
10	0.77	12.5	0.16	0.92
50	0.94	9.56	0.16	1.10
100	1.05	8.15	0.17	1.21
500	2.58	6.48	0.17	2.75

The Schottky diode is electrically similar to a p–n junction, though the current flow in the diode is primarily due to majority carriers having an inherently fast response. It is used extensively for high-frequencies ($f > 500$ kHz). It is very often observed experimentally that the Schottky barrier height calculated from I–V characteristics is not equal to the barrier height extracted from C–V measurements. This is observed especially at low frequencies (for C–V measurements) and nonideal contacts. It is seen that the values of barrier heights higher than the value of the I–V measurements. In conclusion, the Schottky contacts are usually characterized by electrical techniques, most often by I–V or C–V measurements. Both techniques are differently sensitive to possible occurrence of inhomogeneities at the Schottky contact. As the current of the Schottky diode depends exponentially on the barrier height, inhomogeneities and especially small patches with a lower Schottky barrier height (SBH) at the contact, strongly influences the resulting apparent SBH. On the other hand, SBHs calculated from the C–V measurement have a tendency to be an average value of the SBHs of patches present in the contact (barrier height inhomogeneities that are present at the cytosine/n-InP interface), that is, average barrier height is the mean value of the barrier minima plus barrier maxima. In most cases they are higher than the SBH extracted from I–V measurements [50–52]. If the barriers are uniform and ideal, the two measurements yield the same value; otherwise, they will yield different values [47].

4. Conclusion

The barrier heights of the Schottky structures may be tuned by using the thin interlayers of biomolecules. By means of the choice of the organic molecule, the device can be designed to exhibit the desired properties. This study reported here proposes that the cytosine interlayer should be considered, among other candidates, as

a potential thin film for the novel MIS devices. In summary, we have studied as follows: (a) introducing to a new degree of freedom in the control of fundamental device parameters by the inclusion of well-defined cytosine thin interlayer in the Cu/*n*-type InP inorganic MS Schottky diodes, (b) capacitance properties of the device.

References

[1] P. Tran, B. Alavi, G. Gruner, *Phys. Rev. Lett.* **85**, 1564 (2000).

[2] H.-W. Fink, C. Schenenberger, *Nature* **398**, 407 (1999).

[3] S.D. Silaghi, G. Salvan, M. Friedrich, T.U. Kampen, R. Scholz, D.R.T. Zahn, *Appl. Surf. Sci.* **235**, 73 (2004).

[4] D. Porath, A. Bezryadin, S. de Vries, C. Dekker, *Nature* **403**, 635 (2000).

[5] Z. Kutnjak, C. Filipic, R. Podgornik, L. Norgenskiold, N. Korolev, *Phys. Rev. Lett.* **90**, 98101 (2003).

[6] Y. Zhang, R.H. Austin, J. Kraeft, E.C. Cox, P. Ong, *Phys. Rev. Lett.* **89**, 198102 (2002).

[7] Y. Matsuo, G. Kumasaka, K. Saito, S. Ikehata, *Solid State Commun.* **133**, 61 (2005).

[8] V. Kazukauskas, M. Pranaitis, A. Arlauskas, O. Krupka, F. Kajzar, Z. Essaidi, B. Sahraoui, *Opt. Mater.* **32**, 1629 (2010).

[9] O. Krupka, A. El-Ghayoury, I. Rau, B. Sahraoui, J.G. Grote, F. Kajzar, *Thin Solid Films* **516**, 8932 (2008).

[10] J.G. Grote, J.A. Hagen, J.S. Zetts, R.L. Nelson, D.E. Diggs, M.O. Stone, P.P. Yaney, E. Heckman, C. Zhang, W.H. Steier, A.K.-Y. Jen, L.R. Dalton, N. Ogata, M.J. Curley, S.J. Clarson, F.K. Hopkins, *J. Phys. Chem. B* **108**, 8584 (2004).

[11] H.-W. Fink, H. Schmid, E. Ermantraut, T. Schulz, *J. Opt. Soc. Am. A* **14**, 2168 (1997).

[12] R. Czaplicki, O. Krupka, Z. Essaidi, A. El-Ghayoury, F. Kajzar, J.G. Grote, B. Sahraoui, *Opt. Express* **15**, 15268 (2007).

[13] B. Singh, N.S. Sariciftci, J.G. Grote, F.K. Hopkins, *J. Appl. Phys.* **100**, 024514 (2006).

[14] D.D. Eley, D.I. Spivey, *Trans. Faraday Soc.* **58**, 411 (1962).

[15] J. Wang, *Phys. Rev. B* **78**, 245304 (2008).

[16] E. Di Mauro, C.P. Hollenberg, *Adv. Mater.* **5**, 384 (1993).

[17] C.M. Niemeyer, *Angew. Chem. Int. Ed.* **40**, 4128 (2001).

[18] D. Porath, G. Cuniberti, R.D. Felice, *Top. Curr. Chem.* **237**, 183 (2004).

[19] H.M. McConnell, *J. Chem. Phys.* **35**, 508 (1961).

[20] R.E. Holmlin, P.J. Dandliker, J.K. Barton, *Angew. Chem. Int. Ed. Engl.* **36**, 2714 (1997).

[21] C.R. Treadway, M.G. Hill, J.K. Barton, *Chem. Phys.* **281**, 409 (2002).

[22] http://www.worldofmolecules.com/life/cytosine.htm (03.06.2015).

[23] http://en.wikipedia.org/wiki/Cytosine (03.06.2015).

[24] Y. Sakamoto, T. Sugino, T. Miyazaki, J. Shirafuji, *Electron. Lett.* **31**, 1104 (1995).

[25] T. Sugino, H. Ito, J. Shirafuji, *Electron. Lett.* **26**, 1750 (1990).

[26] M.J. Cardwell, R.F. Peart, *Electron. Lett.* **9**, 88 (1973).

[27] O. Gullu, *Microelectron. Eng.* **87**, 648 (2010).

[28] H. Cetin, E. Ayyildiz, A. Turut, *J. Vac. Sci. Technol. B* **23**, 2436 (2005).

[29] R.K. Gupta, R.A. Singh, *J. Polym. Res.* **11**, 269 (2004).

[30] O. Gullu, A. Turut, *Sol. Energy Mater. Sol. Cells* **92**, 1205 (2008).

[31] T.S. Shafai, *Thin Solid Films* **517**, 1200 (2008).

[32] O. Gullu, M. Cankaya, O. Baris, A. Turut, *Appl. Phys. Lett.* **92**, 212106 (2008).

[33] Y. Qiu, J. Qiao, *Thin Solid Films* **372**, 265 (2000).

[34] E.H. Rhoderick, R.H. Williams, *Metal-Semiconductor Contacts*, 2nd ed., Clarendon Press, Oxford 1988.

[35] R.F. Schmitsdorf, T.U. Kampen, W. Monch, *J. Vac. Sci. Technol. B* **15**, 1221 (1997).

[36] F.E. Jones, B.P. Wood, J.A. Myers, C.H. Daniels, M.C. Lonergan, *J. Appl. Phys.* **86**, 6431 (1999).

[37] R.K. Gupta, R.A. Singh, *Mater. Chem. Phys.* **86**, 279 (2004).

[38] A.R.V. Roberts, D.A. Evans, *Appl. Phys. Lett.* **86**, 072105 (2005).

[39] M. Cakar, N. Yildirim, S. Karatas, C. Temirci, A. Turut, *J. Appl. Phys.* **100**, 074505 (2006).

[40] S. Aydogan, M. Saglam, A. Turut, *Microelectron. Eng.* **85**, 278 (2008).

[41] S. Karatas, S. Altindal, A. Turut, M. Cakar, *Physica B* **392**, 43 (2007).

[42] O. Gullu, S. Aydogan, A. Turut, *Microelectron. Eng.* **85**, 1647 (2008).

[43] Ş. Aydoğan, M. Sağlam, A. Türüt, Y. Onganer, *Mater. Sci. Eng. C* **29**, 1486 (2009).

[44] H. Norde, *J. Appl. Phys.* **50**, 5052 (1979).

[45] H.C. Card, E.H. Rhoderick, *J. Phys. D* **4**, 1589 (1971).

[46] O. Gullu, S. Asubay, S. Aydogan, A. Turut, *Physica E* **42**, 1411 (2010).

[47] S. Aydogan, M. Saglam, A. Turut, *Polymer* **46**, 10982 (2005).

[48] A. Turut, N. Yalcin, M. Saglam, *Solid State Electron.* **35**, 835 (1992).

[49] D.A. Vandenbroucke, R.L. Van Meirhaeghe, W.H. Laflere, F. Cardon, *J. Phys. D Appl. Phys.* **18**, 731 (1985).

[50] J. Osvald, *J. Appl. Phys.* **85**, 1935 (1999).

[51] E. Ayyildiz, C. Temirci, B. Bati, A. Türüt, *Int. J. Electron.* **88**, 625 (2001).

[52] S. Asubay, Ö. Güllü, *Int. J. Electron.* **97**, 973 (2010).